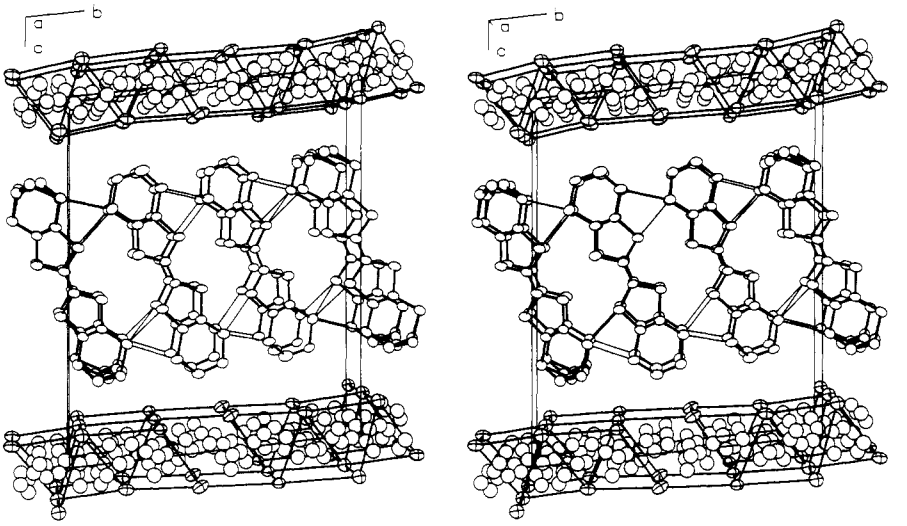

Figure 1. Stereoview of the unit cell of $(ET)_3Ag_xI_8$ ($x \sim 6.4$) along the a axis. The figure shows one layer of the two-dimensional ET donor-molecule network (center) with S···S contacts (3.35–3.65 Å), indicated by thin lines, and two silver iodide layers (top and bottom).

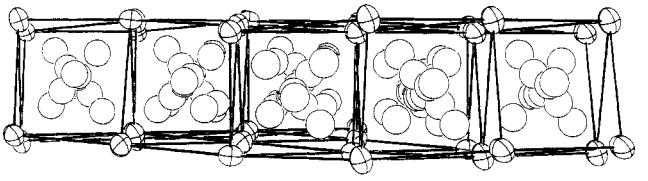

Figure 2. Edge-on view of the silver iodide polyanion layer in $(ET)_3Ag_xI_8$ ($x \sim 6.4$), along $3a + b$. The lines drawn between the iodide ions (with principal ellipses shown) are shorter than 4.65 Å. Silver atom positions within the iodide anion channels are shown as open circles. Similar cation-containing channels are found in numerous solid electrolytes.[10]

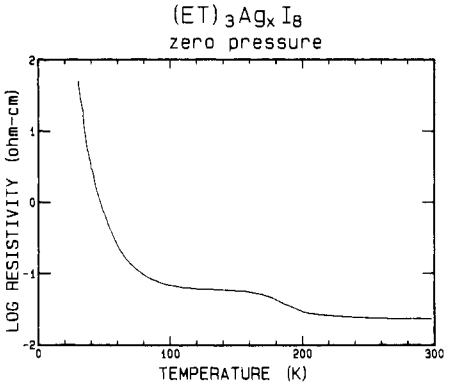

Figure 3. Electrical resistivity (logarithmic scale) along the needle axis (a) of $(ET)_3Ag_xI_8$ ($x \sim 6.4$) as a function of temperature. Metallic conductivity is observed at room temperature ($\sigma \simeq 50\ \Omega^{-1}\ cm^{-1}$).

(1) A dc current (100 μA) was applied for an extended period in order to see polarization effects. No change to within our resolution (0.1%) was observed after 20–30 min. This test assumes that the electrodes are at least partially blocking to ionic transport, a reasonable assumption for the type of contacts we employed. (2) No frequency dependence of the resistivity from 0 to 20 kHz was observed. (3) An uncalibrated heating of one sample above 300 K produced an *increase* in the resistivity, contrary to the expectation for ionic transport. Thus, the electrical conductivity is metallic at room temperature ($\sigma = 50\ \Omega^{-1}\ cm^{-1}$).

Conclusions. $(ET)_3Ag_xI_8$ is the first hybrid synmetal–solid electrolyte. However, the high electrical conductivity is dominated by the electronic contribution, at least near room temperature. This is not surprising, since the highest room-temperature ionic conductivity in silver iodide based solid electrolytes measured is 0.27 $(\Omega\ cm)^{-1}$ in $RbAg_4I_5$.[13,14] Furthermore, even smaller silver ion mobility is expected in $(ET)_3Ag_xI_8$, because the silver ions are confined to parallel channels, whereas transport along all directions is possible in $RbAg_4I_5$. We are currently investigating the nature of the 180 K anomaly and the low-temperature properties of $(ET)_3Ag_xI_8$.

Acknowledgment. Work at Argonne National Laboratory and Sandia National Laboratories is sponsored by the U.S. Department of Energy, Office of Basic Energy Sciences, Division of Materials Sciences, under Contracts W-31-109-Eng-38 and KC020202, respectively.

Supplementary Material Available: Tables of crystal structure data collection and refinement parameters (Table X1) and final atomic positions with anisotropic temperature factors and silver ion occupancy parameters (Tables X2 and X3) (3 pages). Ordering information is given on any current masthead page.

(13) Raleigh, D. O. *J. Appl. Phys.* **1970**, *41*, 1876.

(14) Owens, B. B.; Argue, G. R. *J. Electrochem. Soc.* **1970**, *117*, 898.

(15) K.M.D. and B.A.A. are student research participants sponsored by the Argonne Division of Educational Programs from St. Michael's College, Winooski, VT, and Wittenberg University, Springfield, OH.

Chemistry and Materials Science and Technology Divisions
Argonne National Laboratory
Argonne, Illinois 60439

Urs Geiser
Hau H. Wang
Karen M. Donega[15]
Benjamin A. Anderson[15]
Jack M. Williams*

Sandia National Laboratories
Albuquerque, New Mexico 87185

James F. Kwak

Received December 20, 1985

Molecular Structure of a Nickel(II) Complex with Phenolate-Appended Cyclam

Sir:

The phenol-pendant cyclam **1** was recently synthesized via a novel "recycle" of coumarin with linear the tetraamine 1,9-diamino-3,7-diazanonane.[1] The structurally appropriate positioning of its phenol for apical coordination has been implied by the formation of stable complexes with Fe^{II} and Fe^{III} in aqueous solutions. Furthermore, the phenolate coordination appears to render the higher oxidation state of iron more stable.[1] The new ligand **1** may provide a simplified model for the study of phenolate

(1) Kimura, E.; Koike, T.; Takahashi, M. *J. Chem. Soc., Chem. Commun.* **1985**, 385–386.

0020-1669/86/1325-0402$01.50/0

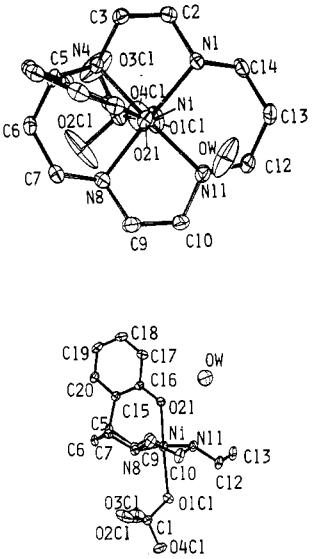

Figure 1. ORTEP[14] drawings of complex **2**. Atoms are drawn with 30% probability ellipsoids. Hydrogen atoms are omitted for clarity. Bond angles are as follows: 85.6 (2)°, N_1–Ni–N_4; 92.0 (2)°, N_1–Ni–O_{21}; 86.0 (2)°, N_1–Ni–O_1(Cl); 96.6 (2)°, N_4–Ni–N_8; 84.9 (2)°, N_8–Ni–N_{11}; 177.6 (2)°, O_{21}–Ni–O_1(Cl); 125.6 (7)°, C_{15}–C_{16}–O_{21}; 126.9 (4)°, Ni–O_{21}–C_{16}.

coordinating effects in biological systems such as tyrosine-coordinating Fe^{III} nonheme oxygenases[2] or apical tyrosine-coordinating hemes.[3,4]

Now we have isolated a Ni^{II} complex of the phenolate-pendant cyclam **2**, which shows a significantly lowered redox potential +0.35 V vs. SCE (0.5 M Na_2SO_4, pH 7.5, 25 °C) for $Ni^{III/II}$ with respect to that (+0.50 V vs. SCE) of Ni^{II}–cyclam complex **3**.[5] This is accounted for by the effect of phenolate apical coordination. The structure of the apical phenolate-pendant cyclam complex **2** is resolved by the present X-ray crystal study. The correlation of high-spin Ni^{II} ion size with the best-fit ring cavity or with the conformation of the macrocyclic tetraamine ligands has been amply investigated.[6-10] However, the present structural parameters of cyclam complex affected by the apical phenolate coordination are the first of this kind to be reported.

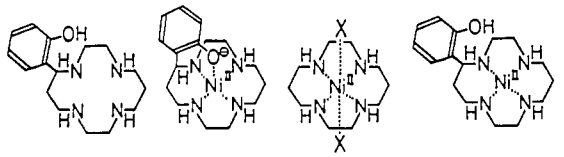

1 2 3 4

The purple crystals of **2** ($C_{16}H_{27}N_4ONiClO_4 \cdot H_2O$) were isolated from a pH 8 aqueous solution of $NiSO_4$ and **1** in the presence of excess $NaClO_4$. They are monoclinic, space group $P2_1$, with a = 16.203 (9) Å, b = 8.042 (5) Å, c = 7.995 (5) Å, β = 104.02 (5)°, Z = 2, and D_c = 1.536 g cm^{-3}, for graphite-monochromated Cu Kα radiation. A total of 2153 structure factors with $I > 2\sigma(I)$ were derived from 2286 intensities collected on a Philips PW1100 diffractometer. The structure was solved by the heavy-atom method and refined by the block-diagonal-matrix least-squares method to an R value of 0.047. Dispersion corrections for C, O, N, Cl, and Ni atoms were applied by taking a set of atomic coordinates that gave a smaller R value. Absorption corrections were not applied. The resulting molecular structure is shown in Figure 1.

Table I. Intermolecular Short Distances (Å)[a]

O_W···O_{21}	2.667 (11)	N_8···O_2(Cl)	3.186 (11)
$H'O_W$···O_{21}	2.19 (11)	HN_8···O_2(Cl)	2.46 (11)
N_{11}···O_W	3.200 (15)	N_1···O_2(Cl)*	3.189 (10)
HN_{11}···O_W	2.42 (9)	HN_1···O_2(Cl)*	2.39 (9)
N_4···O_3(Cl)	3.180 (12)		
HN_4···O_3(Cl)	2.41 (8)		

[a] Atoms marked with an asterisk are at x, y + 1, z; other atoms are at x, y, z.

The five-coordinate, square-pyramidal coordination geometry around nickel is evident. The atoms N_1, N_4, N_8, and N_{11} are coplanar, and the nickel stays in this plane.[11] The phenolate oxygen O_{21} is almost at the apex of the pyramid with the very short apical Ni–O_{21} bond distance 2.015 (5) Å. The previous octahedral high-spin Ni^{II}(cyclam)X_2 complexes **3** showed longer Ni–X apical bonds (2.492 Å for X = Cl,[12] 2.169 Å for X = NO_3[10]). Moreover, the apical Ni–O_{21} bond length is shorter than the equatorial Ni–N bond distances 2.072 (6), 2.051 (5), 2.085 (6), and 2.078 (5) Å for Ni–N_1, –N_4, –N_8, and –N_{11}, respectively. Another apical Ni–O_1(Cl) (of perchlorate) distance is very long at 2.402 (7) Å, indicating a very weak coordinate bond between them. This can be viewed as being a result of a phenolate trans influence. The observed Ni–N bond distances of ~2.07 Å indicate Ni^{II} in the 14-membered macrocyclic tetraamine to be in the high-spin state.[10] In the reported octahedral high-spin Ni^{II}(cyclam)X_2 complexes **3** (X = Cl[12] or NO_3[10]), the Ni–N bond lengths are a little shorter, 2.05–2.06 Å, and were considered to be affected by the steric lengthening of the Ni–X bonds.

The cyclam moiety in **2** takes the normal *trans*-III conformation (i.e. the 1,3-diaminopropane rings have a chair conformation) as in **3**.[10,12] The apical nickel–oxygen–aromatic carbon (Ni–O_{21}–C_{16}) bond angle of 126.9 (4)° is another interesting structural feature. The Dreiding model of **2** indicates that the observed *trans*-III configuration with a Ni–O_{21} bond distance of 2.0 Å and a Ni–O_{21}–C_{16} angle of 127° is the most strain-free structure. This fact in turn suggests that the short apical Ni–O_{21} bond and the coplanar Ni position in the N_4 plane are determined mostly by the ligand steric requirement. The strong apical coordination of the phenolate should contribute to fix Ni^{II} in the high-spin state.[13] Some short intermolecular distances suggesting hydrogen bonding are listed in Table I.

It is of interest to add that the protonation of the coordinated phenolate ion in **2** starts to occur below pH 6 to yield **4**, its pK_a being potentiometrically determined to be 6.30 at 25 °C and I = 0.1 M ($NaClO_4$). Upon protonation, the pendent phenol loses coordinating ability with Ni^{II}. Complex **4** exhibits the $Ni^{III/II}$ redox potential of +0.50 V vs. SCE (0.5 M Na_2SO_4, pH 5.2, 25 °C), the same value as for **3**. Another interesting fact is that upon

(2) Que, L., Jr.; Lipscomb, J. D.; Zimmermann, R.; Münck, E.; Orme-Johnson, N. R.; Orme-Johnson, W. H. *Biochim. Biophys. Acta* **1976**, *452*, 320–334.
(3) Pulsinelli, P. D.; Perutz, M. F.; Nagel, R. L. *Proc. Natl. Acad. Sci. U.S.A.* **1973**, *70*, 3870–3874.
(4) Reid, T. J.; Murthy, M. R. N.; Sicignano, A.; Tanaka, N.; Musick, W. D. L.; Rossmann, M. G. *Proc. Natl. Acad. Sci. U.S.A.* **1981**, *78*, 4767–4771.
(5) Addition of a 10 times excess of phenol to **3** (under the same conditions) does not change the $Ni^{III/II}$ redox potential.
(6) Martin, L. Y.; DeHayes, L. J.; Zompa, L. J.; Busch, D. H. *J. Am. Chem. Soc.* **1974**, *96*, 4046–4048.
(7) Martin, L. Y.; Specrati, C. R.; Busch, D. H. *J. Am. Chem. Soc.* **1977**, *99*, 2968–2981.
(8) Hancock, R. D.; McDougall, G. J. *J. Am. Chem. Soc.* **1980**, *102*, 6551–6553.
(9) Thöm, V. J.; Boeyens, J. C. A.; McDougall, G. J.; Hancock, R. D. *J. Am. Chem. Soc.* **1984**, *106*, 3198–3207.
(10) Thöm, V. J.; Fox, C. C.; Boeyens, J. C. A.; Hancock, R. D. *J. Am. Chem. Soc.* **1984**, *106*, 5947–5955.
(11) It is of interest to point out that in high-spin Ni^{II} complexes with square-pyramidal geometry, the nickel is likely to be raised above the basal N_4 mean plane: e.g. Kushi, Y.; Machida, R.; Kimura, E. *J. Chem. Soc., Chem. Commun.* **1985**, 216–218.
(12) Bosnich, B.; Mason, R.; Pauling, P. J.; Robertson, G. B.; Tobe, M. L. *J. Chem. Soc., Chem. Commun.* **1965**, 97–98.
(13) In aqueous solution μ_{eff} = 2.90 μ_B by the Evans method at 35 °C and I = 0.1 M ($NaClO_4$): Evans, D. F. *J. Chem. Soc.* **1959**, 2003–2005. Without the apical phenolate (i.e. complex **3** under the same conditions) μ_{eff} is found to be lowered to 2.35 μ_B, consistent with its high-spin and low-spin equilibrium in aqueous solution. The same μ_{eff} value was reported for **3** in the literature: Swisher, R. G.; Dayhuff, J. P.; Stuehr, D. J.; Blinn, E. L. *Inorg. Chem.* **1980**, *19*, 1336–1340.

coordination with nickel (in **2**), the phenolate becomes robust toward oxidation, as shown by a shift of the phenolate oxidation potential from ~+0.5 V for uncoordinated **1** at 25 °C and pH 10 to ~+0.9 V vs. SCE for **2**.

Registry No. **2**, 99797-10-1; **4**, 99797-11-2.

Supplementary Material Available: Tables of fractional coordinates and isotropic temperature factors, anisotropic temperature factors, bond lengths, and bond angles (4 pages). Ordering information is given on any current masthead page.

(14) Johnson, C. K. "ORTEP", Report ORNL-3794; Oak Ridge National Laboratory: Oak Ridge, TN, 1965.

Faculty of Pharmaceutical Sciences — **Yoichi Iitaka**
University of Tokyo
Hongo, Bunkyo-ku, Tokyo 113, Japan

Department of Medicinal Chemistry — **Tohru Koike**
Hiroshima University School of Medicine — **Eiichi Kimura***
Kasumi, Hiroshima 734, Japan

Received September 11, 1985

Ferraborane Cluster Chemistry: Reactions of $[(\mu\text{-H})Fe_3(CO)_9BH_3]^-$ with Lewis Bases Leading to Substitution via H_2 Elimination or to Cluster Degradation

Sir:

We have recently characterized the ferraborane cluster $(\mu\text{-H})Fe_3(CO)_9BH_4$ (I')[1] and its conjugate base $[(\mu\text{-H})Fe_3(CO)_9BH_3]^-$ (I).[2] I is a novel example of monoborane supported

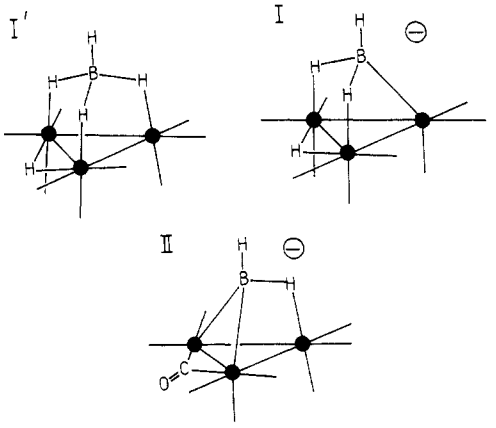

on a multinuclear metal framework and, as such, provokes a study of the competitive interplay between metal and boron cluster sites for association with Lewis bases. The stabilization of BH_3 by Lewis bases is well documented and coordination complexes such as BH_3·THF are commercially available. We wondered if, in I, the BH_3 unit would behave toward Lewis bases, L, in a manner typical of simple BH_3 complexes, thereby being displaced as $L{\cdot}BH_3$ from the cluster, or whether substitution reactions typical of metal carbonyls would predominate. Qualitative investigations of metal carbonyl–ligand substitution reactions far outnumber detailed kinetic studies.[3] The limited data available point toward substitution of the first CO taking place by an associative mechanism for good nucleophilic ligands[3,4] and via a dissociative mechanism for poor nucleophiles.[3-5] The reaction of one metal–boron cluster system with base has been mechanistically examined.[6,7] The study outlined below is an investigation of the reactions of I with Lewis bases of varying nucleophilicity. We show that cluster substitution is via H_2 rather than CO elimination, and only occurs specifically at low ligand concentration. As the concentration of ligand increases, cluster degradation predominates. Kinetic studies evidence an associative mechanism, and we postulate an adduct intermediate that is consistent with the observed reaction products.

Scheme I

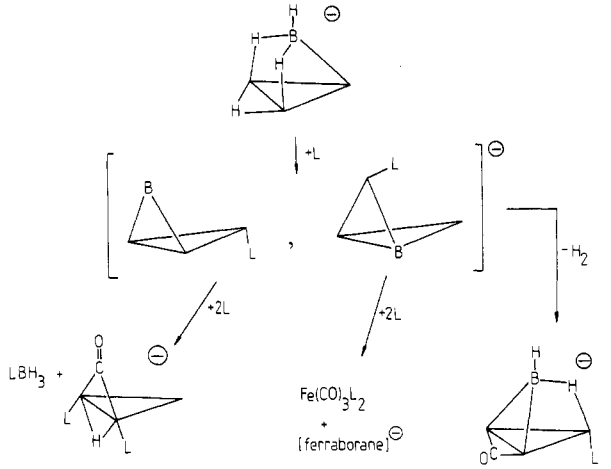

I reacts with CO (1 atm, <1 molar equiv, 45 °C) to form II[2] quantitatively (by NMR) and H_2 is eliminated. Thus, ligand association is with the trimetal frame of I and causes elimination of two skeletal hydrogens thus destroying the integrity of the BH_3 unit but not the integrity of the cluster itself. With excess water (i.e. a Lewis base of low nucleophilicity with respect to a metal but with a strong affinity for boranes), degradation of cluster I occurs, yielding $B(OH)_3$ and $[(\mu\text{-H})Fe_3(CO)_{10}(\mu\text{-CO})]^-$. However, the reaction is markedly slower than the action of H_2O on free BH_3 or on complexed $L{\cdot}BH_3$. With ≥5-fold excess of NEt_3 (a base that coordinates readily to BH_3 but only weakly to metals), I undergoes adduct formation with ≈20% reaction leading to cluster fragmentation, seen by the formation of $Et_3N{\cdot}BH_3$ and $[(\mu\text{-H})Fe_3(CO)_{10}(\mu\text{-CO})]^-$. The evidence for an adduct is spectroscopic,[8] but reversible loss of the amine to regenerate I was observed in our attempts to isolate the species. With a large excess of NEt_3, I is completely fragmented. I reacts with $PhMe_2P$ (a ligand possessing a strong affinity for both metal and boron centers) by three competitive pathways, one substitution and two fragmentation. We have studied this competition in detail and note that the reactions of the aforementioned Lewis bases with I are consistent with the conclusions drawn below.

When I reacts with $PhMe_2P$, the formation of fragmentation vs. substitution products is highly dependent on phosphine concentration. When $PhMe_2P$ is added to a solution of I at levels of <1 molar equiv, the reaction favors substitution with concomitant cluster retention. The product, $[Fe_3(CO)_8(\mu\text{-CO})(PhMe_2P)BH_2]^-$,[9] is a derivative of II, and therefore H_2 elimination

(1) Vites, J.; Eigenbrot, C.; Fehlner, T. P. *J. Am. Chem. Soc.* **1984**, *106*, 4633.
(2) Vites, J. C.; Housecroft, C. E.; Jacobsen, G. B.; Fehlner, T. P. *Organometallics* **1984**, *3*, 1591.
(3) Atwood, J. D. "Inorganic and Organometallic Reaction Mechanisms", Brooks/Cole: Monterey, CA, 1985.
(4) Darensbourg, D. J.; Zalewski, D. J. *Organometallics* **1985**, *4*, 92.
(5) Keister, J. B.; Dalton, D. M.; Smesko, S. A.; Modi, S. P.; Malik, P.; Barnett, D. J.; Duggan, T. P. "Abstracts of Papers", 188th National Meeting of the American Chemical Society, Philadelphia, PA, 1984; American Chemical Society: Washington DC, 1984; INOR 205. Dalton, D. M.; Barnett, D. J.; Duggan, T. P.; Keister, J. B.; Malik, P. T.; Modi, S. P.; Shaffer, M. R.; Smesko, S. A.; *Organometallics* **1985**, *4*, 1854.
(6) Shore, S. G.; Jan, D.-Y.; Hsu, L.-Y.; Hsu, W.-L. *J. Am. Chem. Soc.* **1983**, *105*, 5923.
(7) Jan, D.-Y.; Hsu, L.-Y.; Shore, S. G. "Abstracts of Papers", 188th National Meeting of the American Chemical Society, Philadelphia, PA, 1984; American Chemical Society: Washington, DC, 1984; INOR 180.
(8) In addition to ^{11}B and ^1H NMR spectroscopic changes during the reaction, we observe no H_2 or CO gas evolution by GLC analysis.

0020-1669/86/1325-0404$01.50/0